

# Origin of rubber-like behaviour in metal alloys

Xiaobing Ren & Kazuhiro Otsuka

*Institute of Materials Science, University of Tsukuba, Tsukuba, Ibaraki 305, Japan*

have a high density of defects. It is interesting to compare these defects with flux vortex lattices in superconductivity<sup>20</sup>. At large enough length-scales (above the so-called Larkin length), even arbitrarily weak static defects can destroy translational long-range order for all dimensions  $< 4$ . For flux vortex lattices, the defects are rigidly fixed in space, and not connected to the fluctuating lattice. Long-range order is therefore always destroyed at large enough length-scales. The analogy with smectic elastomers is complex, because the defects are crosslinks which are embedded in the fluctuating lattice itself, and therefore are not strictly static. We observed  $1/q^{2.4}$  intensity tails which persist down to  $q$  values approaching our experimental resolution limit, which is high enough to resolve length-scales of several micrometres. For the limiting case of static crosslinks, the scattering signature may consist of a crossover between the disordered Larkin limit at a small  $q$ , to the predicted Bragg behaviour at large  $q$ , which is the range we observe. As the Larkin length has been known to be macroscopically large even for soft lattices (tens of micrometres) we may not be able to observe this effect even at the high resolution of our experiments. But because crosslinks can locally disturb the smectic layering, and can even destroy the 'one-dimensional' lattice down to molecular length-scales at high crosslink densities<sup>21</sup>, the lineshape at our measured range of  $q$  values can also be affected. As with effects related to the mosaic width, such defects can only broaden rather than sharpen the lineshape associated with the 'one-dimensional' ordering, and therefore cannot explain our unambiguous observation of an elastomer Bragg peak that is sharper than the Caillé lineshape. In these smectic elastomers the introduction of disorder in the form of a random network has the counterintuitive result of enhancing the 'one-dimensional' ordering. □

Received 29 November 1996; accepted 15 August 1997.

- Landau, L. D. in *Collected Papers of L. D. Landau* (ed. ter Haar, D.) 193–216 (Gordon & Breach, New York, 1965).
- Peierls, R. E. Bemerkung über Umwandlungstemperaturen. *Helv. Phys. Acta Suppl.* **7**, S81–S83 (1934).
- Chaikin, P. M. & Lubensky, T. C. *Principles of Condensed Matter Physics* (Cambridge Univ. Press, New York, 1995).
- de Gennes, P. G. & Prost, J. *The Physics of Liquid Crystals* 2nd edn (Clarendon Press, Oxford, 1993).
- Safinya, C. R. *et al.* Steric interactions in a model multimembrane system: a synchrotron X-ray study. *Phys. Rev. Lett.* **57**, 2718–2721 (1986).
- Sirota, E., Smith, G. S., Safinya, C. R., Plano, R. J. & Clark, N. A. X-ray scattering studies of aligned, stacked surfactant membranes. *Science* **242**, 1406–1409 (1988).
- Als-Nielsen, J. *et al.* Observation of algebraic decay of positional order in a smectic liquid crystal. *Phys. Rev.* **B22**, 312–320 (1980).
- Nachaliel, E., Keller, E. N., Davidov, D. & Boeffel, C. Algebraic dependence of the structure factor and possible anharmonicity in a high resolution X-ray study of a side-group polymeric liquid crystal. *Phys. Rev.* **A43**, 2897–2902 (1991).
- Zentel, R. Liquid crystalline elastomers. *Angew. Chem. Adv. Mater.* **101**, 1407–1415 (1989).
- Finkelmann, H., Benne, J. & Semmler, K. Smectic liquid crystal elastomers. *Macromol. Symp.* **96**, 169–174 (1995).
- Terentjev, E. M., Warner, M. & Lubensky, T. C. Fluctuations and long-range order in smectic elastomers. *Europhys. Lett.* **30**, 343–348 (1995).
- Caillé, A. Remarques sur la diffusion des rayons X dans les smectiques. *C. R. Acad. Sci. Paris* **B274**, 891–893 (1972).
- Warren, B. E. *X-ray Diffraction* (Addison-Wesley, Reading, 1969).
- de Gennes, P. G. in *Polymer Liquid Crystals* (eds Ciferri, A., Krigbaum, W. R. & Meyer, R. B.) 115–132 (Academic, New York, 1982).
- Mitchell, G. R., Davis, F. J. & Guo, W. Strain-induced transitions in liquid-crystal elastomers. *Phys. Rev. Lett.* **71**, 2947–2950 (1993).
- Krivoglaz, M. *Theory of X-ray and Thermal Neutron Scattering by Real Crystals* (Plenum, New York, 1969).
- Zentel, R. & Benalia, M. Stress-induced orientation in lightly crosslinked liquid-crystalline side-group polymers. *Makromol. Chem.* **188**, 665–674 (1987).
- Kaganer, V. M., Ostrovsky, B. I. & de Jeu, W. H. X-ray scattering in smectic liquid crystals: from ideal to real-structure effects. *Phys. Rev.* **A44**, 8158–8166 (1991).
- Olmsted, P. D. & Terentjev, E. M. Mean-field nematic-smectic-A transition in a random polymer network. *Phys. Rev.* **E53**, 2444–2453 (1996).
- Blatter, G., Feigelman, M. V., Geshkenbein, V. B., Larkin, A. I. & Vinokur, V. M. Vortices in high temperature superconductors. *Rev. Mod. Phys.* **66**, 1125–1380 (1994).
- Terentjev, E. M. Non-uniform deformations and molecular random fields in liquid crystalline elastomers. *Macromol. Symp.* **117**, 79–88 (1997).

**Acknowledgements.** We thank E. M. Terentjev for discussions, E. Gebhard for assistance in sample preparation, and J. Commandeur for technical support. This work is part of the research program of the Stichting voor Fundamenteel Onderzoek der Materie [Foundation for Fundamental Research on Matter (FOM)] with support from the Nederlandse Organisatie voor Wetenschappelijk Onderzoek [Netherlands Organization for the Advancement of Research (NWO)]. W.d.J. acknowledges additional support from a NATO collaborative research grant.

Correspondence and requests for materials should be addressed to W.H.d.J. (e-mail: dejeu@amolf.nl)

Since 1932 it has been known that a number of ordered alloys show an unusual kind of deformation behaviour<sup>1–3</sup>. These alloys (including Au–Cd, Au–Cu–Zn, Cu–Zn–Al, Cu–Al–Ni)<sup>4–8</sup>, after being aged for some time in a martensitic state (the low-symmetry phase of a diffusionless transformation), can be deformed like a soft and pseudo-elastic rubber (with a recoverable strain as large as a few per cent). Accompanying martensite ageing is the development of martensite stabilization<sup>9</sup> (increase in the temperature of reverse transformation to the parent state), the avoidance of which is important in actuator applications of the shape-memory effect<sup>29</sup>, (which these alloys also generally exhibit). The origin of this rubber-like behaviour and of the ageing effect has remained unclear<sup>10–17</sup>. Here we show that this behaviour does not involve a change in the degree of long-range order, but is instead due to an atomic rearrangement within the same sub-lattice of the imperfectly ordered alloy during martensite ageing. This process is driven by a general tendency for the equilibrium symmetry of the short-range order configuration of lattice imperfections to conform to the symmetry of the lattice. This principle not only explains all the observed aspects of the rubber-like behaviour and the ageing effect in both ordered and disordered alloys, but may also further our understanding of some diffusion phenomena in other crystalline materials.

A martensitic transformation lowers the symmetry of a crystal without involving atomic exchange or diffusion. As a result of symmetry lowering, a single crystal of the parent phase (high-temperature phase) is split into many twin-related martensite domains. If the martensite of the above-mentioned alloys is deformed immediately after being transformed from the parent phase, the strain can be accommodated by the easy reversal of some of the domains into new ones, that is, twinning. This explains the 'softness' of the martensite. Because the stress-induced domains have the same martensite structure and hence the same stability as

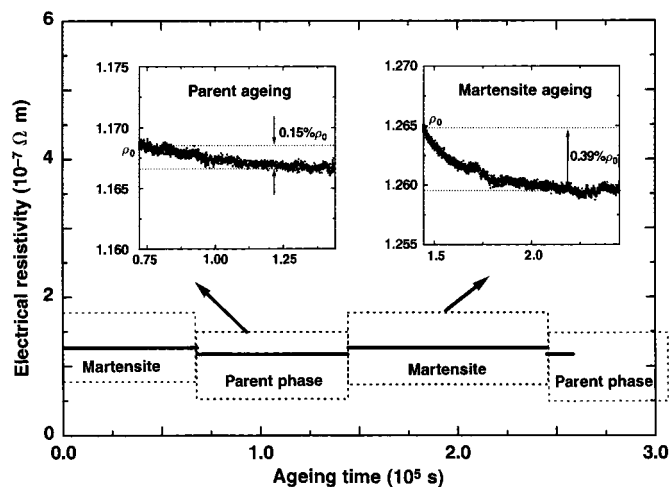


**Figure 1** Electrical resistivity of single crystal Au<sub>50.5</sub>Cd<sub>49.5</sub> alloy as a function of ageing time, for the parent phase (enlarged in the left inset) after transformation from well-aged martensite, and for martensite (enlarged in the right inset) after transformation from well-aged parent.

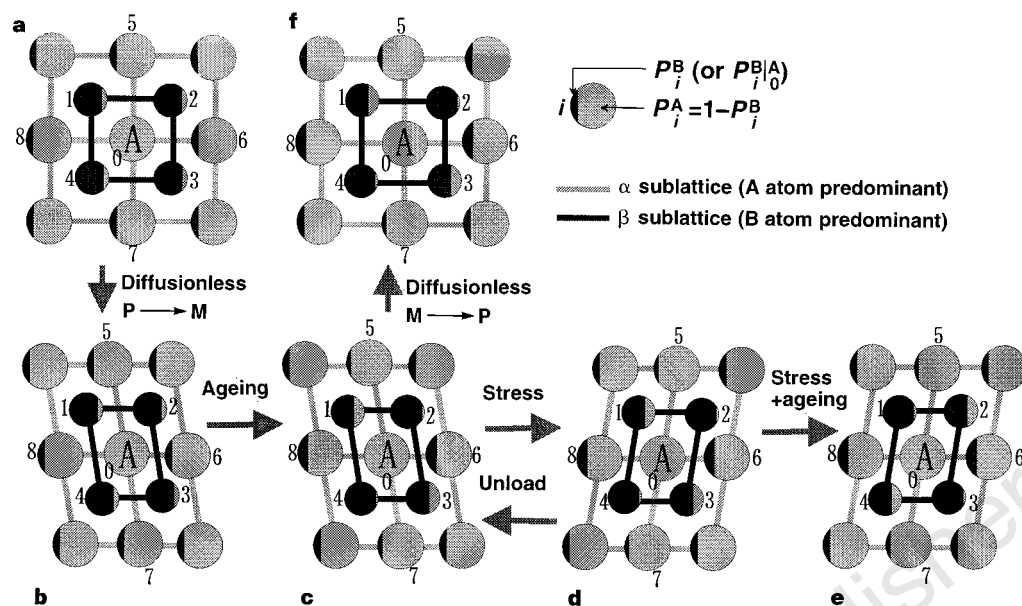


**Figure 2** Mechanism of rubber-like behaviour and the martensite stabilization phenomenon. The illustrations show the statistical atomic configuration (conditional probabilities around an A atom) of an imperfectly-ordered A–B alloy in: **a**, the equilibrium parent phase; **b**, the martensite immediately after transformation from **a**; **c**, the equilibrium martensite; **d**, the stress-induced martensite domain (twin) formed immediately from **c**; **e**, the equilibrium state of the stress-induced domain; **f**, the parent transformed immediately from **c**. P, parent phase; M, martensite.  $P_i^B$  (or  $P_i^A$ ) is the conditional probability of a B atom (or an A atom) occupying site  $i$  ( $i = 1, 2, 3, \dots, 8$ ) if an A atom is at site 0. The relative values of  $P_i^B$  and  $P_i^A$  are indicated by the black and grey areas respectively.

the original ones, the original domains cannot be restored even when stress is released. This leads to a plastic or irrecoverable strain for the ‘fresh’ martensite.

However, the rubber-like behaviour appears when martensite is deformed after being aged for a certain period. Then the stress-induced domains seem to be less stable than the original ones, so the original domains can be restored when the stress is removed. This leads to a recoverable strain and to macroscopic rubber-like behaviour (RLB). The central problem is to explain what happens during martensite ageing to cause the stability difference between the stress-induced domain and the original one. RLB is different from two other kinds of pseudoelasticity of known origin. One is due to stress-induced martensitic transformation<sup>1</sup>, and the other is due to the formation of a pseudo-twin<sup>18</sup>. In both cases, stress induces a structural transformation that provides the restoring force.

The existence of RLB in single-domain martensites<sup>19,20</sup> proved that RLB and the ageing effect must originate from atomic rearrangement throughout the martensite. Previous martensite reconstruction models<sup>11,12</sup> were found to contradict experimental observations<sup>21</sup>. Recent models<sup>13–17</sup> also predicted some change in the average martensite structure (that is, the degree of long-range order (LRO)) during ageing. However, X-ray experiments on stable (that is, no tendency to decompose) Au–Cu–Zn<sup>22</sup> and Au–Cd<sup>20,21</sup> martensites did not provide any evidence for a change in the degree of LRO, but with a relatively large uncertainty (a few per cent).

Here we present experimental evidence to show that no change in LRO occurs during ageing. Because of the great sensitivity of electrical resistivity to changes in LRO in alloys, we used a four-terminal electrical resistivity measurement to monitor the possible LRO change during isothermal ageing for a Au<sub>50.5</sub>Cd<sub>49.5</sub> ordered alloy in a consecutive ageing sequence: martensite (298 ± 0.2 K for ~2 × 10<sup>5</sup> s) → parent (330 ± 0.2 K for ~10<sup>5</sup> s) → martensite (298 ± 0.2 K for ~10<sup>5</sup> s). The result is shown in Fig. 1. Notably, both the parent and the martensite show a small decrease in resistivity (relaxation type) with ageing time before reaching saturation. Because diffusionless martensitic transformation does not change LRO, no change in LRO will occur during ageing if the parent and martensite have the same equilibrium LRO. If they were different, one would expect an increase in LRO in one phase and a decrease in the other during ageing, and consequently a remarkable decrease in resistivity in one phase and an increase in the other. This situation obviously contradicts the experimental observation, so we can conclude that no

LRO change is involved during ageing and that the small decrease in resistivity of both phases during ageing is due to a type of relaxation process that does not change LRO.

There is only one type of atomic rearrangement that does not change the degree of LRO: atomic rearrangement within the same sublattice of the ordered martensite, not between sublattices. This process is similar to the atomic diffusion process in ordered alloys, where effective (or net) atomic exchange occurs only within the same sublattice so as not to destroy the LRO<sup>23</sup>. We show below that such an atomic rearrangement has a simple origin.

To simplify the discussion, we consider a two-dimensional structure. However, the conclusion is applicable to any three-dimensional martensite structure because only symmetry is relevant. Fig. 2a shows a two-dimensional A–B binary imperfectly ordered parent phase with four-fold symmetry. Because of the four-fold symmetry of the structure, the probability of finding a B atom about the A atom (or B atom) must possess the same four-fold symmetry (if not, four-fold crystal symmetry cannot be maintained), that is,  $P_1^B = P_2^B = P_3^B = P_4^B$ ,  $P_5^B = P_6^B = P_7^B = P_8^B$ , and so on, where  $P_i^B$  ( $i = 1, 2, 3, \dots$ ) are conditional probabilities, as explained in Fig. 2. The martensite has a lower symmetry, so the equilibrium occupation probability of atoms should also have the same symmetry as the structure about the A atom, that is,  $P_1^B = P_3^B \neq P_2^B = P_4^B$  and  $P_5^B = P_7^B \neq P_6^B = P_8^B$ , as shown in Fig. 2c. The equalities are due to the centro-symmetry of the schematic martensite structure.

Now, let the parent phase shown in Fig. 2a transform into martensite. Because of the diffusionless nature of the transformation, all the probabilities must remain unchanged despite the symmetry change, as shown in Fig. 2b. That is,  $P_1^B = P_2^B = P_3^B = P_4^B$  and  $P_5^B = P_6^B = P_7^B = P_8^B$ , and so on. But this high-symmetry configuration is no longer a stable configuration for the lower-symmetry martensite structure. Then during ageing, such a configuration gradually changes into the stable one, as shown in Fig. 2c. This process proceeds by atomic rearrangement or relaxation within the same sublattice. This is the only way that a martensite can lower its free energy without altering the average martensite structure (equilibrium phase). It is obvious that such an atomic rearrangement occurs most easily for the atoms close to the A atom (for example, atoms 1–8 shown in Fig. 2), and farther atoms make only a small contribution. This means that it is a type of short-range ordering (SRO) within the same sublattice. As shown above, this SRO originates from a requirement that the symmetry of the configuration of lattice imperfections in equilibrium conforms to

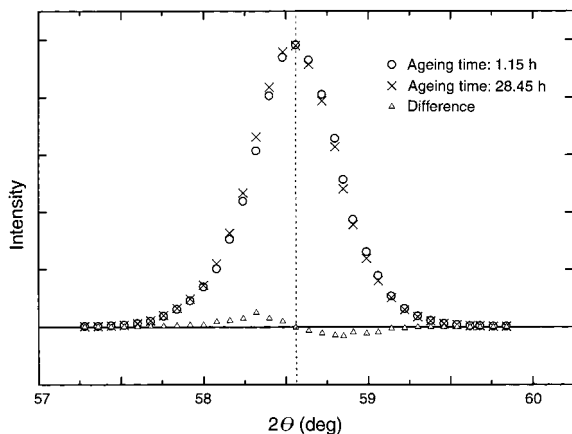


**Figure 3** X-ray profiles of (242) Bragg reflection of single-crystal Au<sub>52.5</sub>Cd<sub>47.5</sub> martensite after ageing for a short (1.15 h) and a long (28.45 h) time<sup>21</sup>. No perceptible change in peak position and integrated intensity was found during ageing. However, a delicate change in the symmetry of the profile was found to develop during ageing, as shown by the difference in the two profiles.

the crystal symmetry and is thus called symmetry-conforming short-range ordering. The stable SRO configuration for the parent is inherited by martensite during martensite formation, but this SRO becomes an 'unstable' configuration for the martensite because it differs from the martensite symmetry. Then atomic rearrangement occurs during ageing that results in a correct SRO symmetry for the martensite. This SRO is apparently different from previously proposed ones<sup>15–17</sup> that lead to a change in LRO.

When the stabilized (or aged) martensite (Fig. 2c) is deformed, it changes into another domain (or twin) as a result of the accommodation of the strain. Because this twinning process is also diffusionless, the atomic occupation probabilities shown in Fig. 2c are inherited by the new domain, as shown in Fig. 2d, but this configuration is not stable for the new domain, which is shown in Fig. 2e, and a driving force that tries to restore the original domain (Fig. 2c) develops. When the external stress is released immediately after loading, this restoring force restores the new domain (Fig. 2d) to the original one (Fig. 2c) by de-twinning. By this mechanism the aged martensite can be deformed like a rubber. We propose that this is the origin of the RLB. If the stress is held for some time, the atomic configurations in Fig. 2d have enough time to change into a stable configuration (Fig. 2e), so no RLB occurs. This has also been found in previous experiments<sup>11,20</sup>. It should be emphasized that this mechanism makes use of only two main features of the martensitic transformation—symmetry change and absence of diffusion—which are shared by all martensites. Thus it is a general mechanism applicable to any martensite.

When the stabilized martensite (Fig. 2c) is heated and transformed back (diffusionlessly) into the parent, the stable SRO configuration for the martensite is inherited by the parent (Fig. 2f). From the above-mentioned symmetry-conforming principle of SRO, it is obvious that Fig. 2f is not a stable configuration for the parent. From a thermodynamic point of view this corresponds to an increased reverse transformation temperature (known as  $A_s$ ). This is the origin of the so-called martensite stabilization<sup>9</sup>, which has previously had no unified explanation.

The present model can be easily extended into disordered alloys by considering the existence of only one sublattice. In this case the present model reduces to Christian's model<sup>24</sup>, which was later elaborated by Otsuka and Wayman<sup>1</sup>. This model explained the rubber-like elasticity in disordered alloys such as In–Ti<sup>25,26</sup>.

We are able to verify the present model directly by comparing it with published X-ray diffraction measurements<sup>21</sup> (Fig. 3). The invariance of the Bragg peak position (that is, lattice parameters)

and intensity indicates that atomic rearrangement during ageing does not change the average structure or LRO of martensite. The small change in shape of the Bragg peak with ageing reflects a delicate change in the environment of a given atom from Fig. 2b to Fig. 2c. Such a change leads to a small change in displacement field around a given atom, and results in a change in the shape of Bragg peaks. The change of the Bragg peak symmetry shows that the SRO configuration changes into the same symmetry as the martensite (the atomic structure of Au–Cd martensite is asymmetrical). The same result was also found in Au<sub>50.5</sub>Cd<sub>49.5</sub> (ref. 20) and Au–Cu–Zn (ref. 22) alloys. So we can see that all of these previously unexplained experimental observations support the present model. The small decrease in resistivity in both martensite and the parent phase (Fig. 1) also provides support for the above mechanism, as it corresponds to the 'fine adjustment' or 'relaxation' within the same sublattice of the ordered structure after a sudden change in symmetry.

From Fig. 2 one can easily see that if there is perfect ordering, no lattice imperfections exist and thus there is no symmetry-conforming short-range ordering of imperfections. Thus, the existence of lattice imperfection is a necessary condition for the ageing effect and RLB. It follows that the more imperfections there are, the more pronounced is the effect. Experimentally<sup>5</sup>, it has been reported that the deviation from stoichiometry (increase in imperfections) in Au–Cd compounds markedly enhances RLB and the ageing effect, and quenching (increase in imperfections) always promotes RLB and the ageing effect.

Behind the above explanation of RLB and the ageing phenomenon is a principle of potentially more general significance: the symmetry-conforming principle of SRO. We believe that this principle is a key to understanding a wide spectrum of diffusion phenomena after a forced symmetry change either by a diffusionless transition or by an external field. RLB and the stabilization effect, as well as Zener ordering<sup>27,28</sup> (due to a symmetry change by an external field), are just a few examples of this common origin. □

Received 19 May; accepted 29 July 1997.

- Otsuka, K. & Wayman, C. M. in *Review on the Deformation Behavior of Materials* Vol. 2 (ed. Feltham, P.) 81–172 (Freund, Tel Aviv, Israel, 1977).
- Christian, J. W. Deformation by moving interface. *Metall. Trans.* **13A**, 509–538 (1982).
- Cahn, R. W. Metallic rubber bounces back. *Nature* **374**, 120–121 (1995).
- Ölander, A. An electrochemical investigation of solid cadmium–gold alloys. *J. Am. Chem. Soc.* **56**, 3819–3833 (1932).
- Nakajima, Y., Aoki, S., Otsuka, K. & Ohba, T. The rubber-like behavior of ζ' (trigonal) martensite in Au–49.5 to 50.0 at% Cd alloys. *Mater. Lett.* **21**, 271–274 (1994).
- Miura, S., Maeda, S. & Nakanishi, N. Pseudoelasticity in Au–Cu–Zn thermoelastic martensite. *Phil. Mag.* **30**, 565–581 (1974).
- Rapacioli, R., Chandrasekaran, M. & Ahlers, M. in *Shape Memory Effects in Alloys* (ed. Perkins, J.) 365–378 (Plenum, New York, 1975).
- Sakamoto, H., Otsuka, K. & Shimizu, K. Rubber-like behavior in a Cu–Al–Ni alloy. *Scripta Metall.* **11**, 607–611 (1977).
- Tadaki, K., Otsuka, K. & Shimizu, K. Shape memory alloys. *Annu. Rev. Mater. Sci.* **18**, 25–45 (1988).
- Birnbaum, H. K. & Read, T. A. Stress induced twin boundary motion in AuCd β' and β'' alloys. *Trans. AIME* **218**, 662–669 (1960).
- Lieberman, D. S., Schmetling, M. A. & Karz, R. S. in *Shape Memory Effects in Alloys* (ed. Perkins, J.) 203–244 (Plenum, New York, 1975).
- Zangwill, A. & Bruinsma, R. Origin of martensitic pseudoelasticity. *Phys. Rev. Lett.* **53**, 1073–1076 (1984).
- Abu Arab, A. & Ahlers, M. The stabilization of martensite in Cu–Zn–Al alloys. *Acta Metall.* **36**, 2627–2638 (1988).
- Tadaki, K., Okazaki, H., Nakata, Y. & Shimizu, K. Atomic configuration studies by ALCHEMI and X-ray diffraction of a stabilized M18R martensite in a β phase Cu–Au–Zn alloy. *Mater. Trans. Jpn Inst. of Metals* **31**, 941–947 (1990).
- Ahlers, M., Barcelo, G. & Rapacioli, R. A model for the rubber-like behavior in Cu–Zn–Al martensites. *Scripta Metall.* **12**, 1075–1078 (1978).
- Marukawa, K. & Tsuchiya, K. Short-range ordering as the cause of the rubber-like behavior in alloy martensites. *Scripta Metall.* **32**, 77–82 (1995).
- Suzuki, T., Tonokawa, T. & Ohba, T. Role of short-range order in martensitic transformation. *J. Phys. III* **5**(C8), 1065–1070 (1995).
- Cahn, J. W. Thermodynamic and structural changes in deformation twinning of alloys. *Acta Metall.* **25**, 1021–1026 (1977).
- Barcelo, G., Rapacioli, R. & Ahlers, M. The rubber effect in Cu–Zn–Al martensite. *Scripta Metall.* **12**, 1069–1074 (1978).
- Murakami, Y., Nakajima, Y., Otsuka, K. & Ohba, T. Effect of existing twin boundaries in martensite on the rubber-like behavior and aging effect in Au–Cd alloys. *J. Phys. III* **5**(C8), 1071–1076 (1995).
- Ohba, T., Otsuka, K. & Sasaki, S. Study of rubber-like behavior in an Au–47.5 at% Cd alloy by synchrotron-orbital radiation. *Mater. Sci. Forum* **56–58**, 317–322 (1990).
- Ohba, T., Finlayson, T. & Otsuka, K. Diffraction profile change in Au–Cu–Zn alloy with aging. *J. Phys. III* **5**(C8) 1083–1086 (1995).
- Hagel, W. C. in *Intermetallic Compounds* (ed. Westbrook, J. H.) 377–404 (Wiley, New York, 1967).
- Christian, J. W. *The Theory of Transformations in Metals and Alloys* (Pergamon, Oxford, 1965).

25. Burkart, M. W. & Read, T. A. Diffusionless phase change in the indium–thallium system. *Trans. AIME* **197**, 1516–1523 (1953).
26. Basinski, Z. S. & Christian, J. W. Crystallography of deformation by twin boundary movement in indium–thallium alloys. *Acta Metall.* **2**, 101–116 (1954).
27. Zener, C. Stress induced preferential orientation of pairs of solute atoms in metallic solid solution. *Phys. Rev.* **71**, 34–38 (1947).
28. Birkenbeil, H. J. & Cahn, R. W. Induced magnetic anisotropy created by magnetic and stress annealing of iron–aluminium alloys. *Proc. Phys. Soc.* **79**, 831–847 (1962).
29. Miyazaki, S. & Otsuka, K. in *Shape Memory Alloys* (ed. Funakubo, H.) 116–175 (Gordon and Breach, New York, 1987).

**Acknowledgements.** We thank T. Suzuki, T. Ohba, H. Horiuchi, M. Kogachi and Y. Murakami for helpful discussions and critical reading the manuscript; T. Ishii for technical assistance; and T. Ohba for allowing us to use his published diffraction data. The work was supported by a Grant-in-Aid for Scientific Research on Priority Area of Phase Transformations (1997–1999) from the Ministry of Education, Science and Culture of Japan. X.R. is a recipient of a JSPS Fellowship.

Correspondence and requests for materials should be addressed to K.O. (e-mail: otsuka@mat.ims.tsukuba.ac.jp).

## Bending and buckling of carbon nanotubes under large strain

M. R. Falvo\*, G. J. Clary†, R. M. Taylor II†, V. Chi†, F. P. Brooks Jr†, S. Washburn\* & R. Superfine\*

\* Department of Physics and Astronomy, † Department of Computer Science, University of North Carolina, Chapel Hill, North Carolina 27599, USA

The curling of a graphitic sheet to form carbon nanotubes<sup>1</sup> produces a class of materials that seem to have extraordinary electrical and mechanical properties<sup>2</sup>. In particular, the high elastic modulus of the graphite sheets means that the nanotubes might be stiffer and stronger than any other known material<sup>3–5</sup>, with beneficial consequences for their application in composite bulk materials and as individual elements of nanometre-scale devices and sensors<sup>6</sup>. The mechanical properties are predicted to be sensitive to details of their structure and to the presence of defects<sup>7</sup>, which means that measurements on individual nanotubes are essential to establish these properties. Here we show that multiwalled carbon nanotubes can be bent repeatedly through large angles using the tip of an atomic force microscope, without undergoing catastrophic failure. We observe a range of responses to this high-strain deformation, which together suggest that nanotubes are remarkably flexible and resilient.

Two mechanical properties of a material are of principal interest here: the small-strain elastic modulus and the material strength. The basal-plane elastic modulus of graphite, the largest of any known material, confers on the nanotube its predicted extraordinary stiffness<sup>3,4,24</sup>. These expectations are consistent with reports of transmission electron microscope (TEM) measurements taken in the small-strain limit<sup>5</sup>, and atomic force microscope (AFM) measurements which were extended beyond the linear elastic regime<sup>8</sup>. Although the high stiffness is predicted to provide an improvement over existing materials, it is the nanotube's unusual strength which is its most distinguishing property. The unusual strength arises from the high stiffness, expected to be consistent with the modulus of graphite, combined with extraordinary flexibility and resistance to fracture. It is this latter feature which will distinguish nanotubes from graphitic fibres as an engineering material. Two theoretical approaches to understanding and predicting the large-strain behaviour of carbon nanotubes are atomistic molecular-dynamics simulations and continuum mechanics. The remarkable correspondence between the two approaches and TEM observations has been appreciated recently in the case of the smallest single- and double-wall tubes under flexural strains which produce buckling deformations<sup>9</sup>. Large multiwalled nanotubes (MWNTs) present challenges to both theoretical approaches in that molecular-dynamics simulations are limited in the size of the system that can be modelled, and continuum mechanics has been most successful in the thin-shell limit.

Knowledge of the large-strain behaviour of carbon nanotubes relies largely on the TEM observations of as-deposited, small-diameter tubes. Typically, many small kinks are seen on the compressed side of an otherwise smooth bend in a MWNT<sup>10,11</sup>; molecular-dynamics simulations predict this kinking to be reversible even under very severe bending<sup>12</sup>. This is consistent with indirect evidence of reversible buckling of a carbon nanotube while attached to an AFM probe<sup>8</sup>. This indicates a fibre of unusual strength. Until now, experimental evidence of the structure of bent nanotubes has relied largely on finding nanotubes which have been bent either during the deposition procedure or through the distortion of the substrate<sup>13,14</sup>. Ideally, experiments should be performed where the full history of the strain, including the initial condition of the tube and the reversibility of the structure, is known. Using a unique interface for atomic force microscopes, we have performed intricate bending of MWNTs to large strains.

Samples were prepared by solvent evaporation on mica substrates of an ethanol solution of raw carbon soot (produced from the carbon-arc technique<sup>15</sup>). The carbon nanotubes were imaged and manipulated under ambient conditions. The 'Nanomanipulator' AFM system, designed for manipulation, comprises an advanced visual interface, teleoperation capabilities for manual control of the AFM tip and tactile presentation of the AFM data (Discoverer, Topometrix Inc., Santa Clara, CA)<sup>16,17</sup>. Initially, the tubes are straight with no apparent structural defects. The AFM tip is used to apply lateral stresses at locations along the tube to produce translations and bends. The friction between the tube and the substrate pins the tube in its strained configuration for imaging. On some samples, however, the tube/substrate friction is too low to maintain the highly strained nanotube, and relaxation of the tube is observed during AFM imaging.

A carbon nanotube, pinned at one end by carbon debris, was bent into many configurations. The inset of Fig. 1a shows the tube in its original adsorbed position and orientation. The abrupt vertical step on the left side of the tube was used as a reference mark ( $s = 0$ , where  $s$  is the measured distance along the tube centre line) for feature locations. The nanotube was taken through a series of 20 distinct manipulations, alternately bending and straightening the tube at various points. We present images from this sequence to highlight specific features (Fig. 1a–d). Along with AFM topographic data, we also show the tube height along the tube's centre as determined by the cores method<sup>18,19</sup>, along with the calculated curvature (Fig. 1e–h). We will refer to raised points on the tube as 'buckles', consistent with the increase in height expected from the collapse of a shell in response to bending. We observe two behaviours in this sequence: small, regularly distributed buckles at regions of small curvature and large deformation at high curvatures.

We focus first on the regularly spaced buckles occurring in the more gradually bent region (Fig. 1a, lower right). Figure 1b and c shows the tube as it is bent in opposite directions. The location of the buckles has shifted dramatically, with the buckles of Fig. 1c appearing in regions which had been featureless, and the buckles of Fig. 1b largely disappearing. The buckles appear with a characteristic interval independent of their absolute position along the tube. This suggests the buckling is reversible, intrinsic to the nanotube and not mediated by defects. The strong correlation between tube curvature and the location of buckles confirms their role in reducing curvature-induced strain. Buckling in bent shells are well known in continuum mechanics<sup>20</sup> where two modes of deformation result from pure bending stresses. The Brazier effect causes the circular cross-section of the tube to become more 'ovalized' uniformly over the whole tube length<sup>21</sup> as the bending curvature increases. Bifurcation, on the other hand, leads to a periodic, low-amplitude rippling of the tube wall on the inside of the bend (the portion under compression). Experiment and theory show<sup>21</sup> that both modes often occur simultaneously, and lead to single-kink collapse as the bending moment reaches its maximum critical value. The axial